EPTT 2024
Escola de Primavera de Transição e Turbulência

ABCM
Associação Brasileira de Engenharia e Ciências Mecânicas

EPTT-2024-0024
ANALYSIS OF EXTREME EVENTS IN THE BOUNDARY LAYER OF A NACA0012 AT HIGH ANGLE OF ATTACK

Leandro Júnio de O. Silva
William R. Wolf
Universidade Estadual de Campinas, Campinas, SP, 13083-860, Brazil
l184929@dac.unicamp.br, wolf@fem.unicamp.br

Abstract. *We investigate the effects of adverse pressure gradients (APGs) on extreme events in the turbulent boundary layer (TBL) of a NACA0012 airfoil at* 9 *deg. angle of attack. A wall-resolved large-eddy simulation (LES) is performed for a Reynolds number* $Re = 4 \times 10^5$ *and freestream Mach number* $M = 0.2$*. Boundary layer tripping is enforced near the leading edge to have bypass transition. Despite the high angle of attack, the mean flow remains attached over the airfoil suction side, although the adverse pressure gradient exhibits a steep rise towards the trailing edge. Results of a quadrant analysis for the Reynolds shear stress distribution show that sweeps are predominant near the wall, while ejections dominate in the outer region.*
Keywords: *turbulent boundary layer, adverse pressure gradient, extreme events*

1. INTRODUCTION

Airfoil profiles are found in wings, propellers, rotorcraft and wind turbines. For most of such applications, turbulent boundary layers (TBLs) develop over the airfoils and their envelope of application may span conditions with high angles of attack, where the TBLs are subject to strong pressure gradients. Turbulent boundary layers may also contain intermittent features associated with coherent motion (Ricciardi *et al.*, 2022) which can affect transition to turbulence and noise generation. Such extreme events have been analyzed in the past concerning bursts associated with powerful ejections of fluid transported away from the wall (Willmarth and Lu, 1972).

Extreme events leave traces that can be observed, for example, by large values of skewness in a probability density function (PDF) (Farazmand and Sapsis, 2017). In order to characterize extreme events, Wallace *et al.* (1972) and Lu and Willmarth (1973) proposed a quadrant splitting analysis in terms of the instantaneous Reynolds shear stress. In this analysis, the second and forth quadrants are related to ejections and sweeps, respectively, whereas the first and third quadrant represent outward and inward interactions. The application of this methodology was performed by Schatzman and Thomas (2017) to investigate the role of extreme events in unsteady turbulent boundary layers. The authors conducted experiments to analyze APG-TBLs where the pressure gradient was time dependent. They demonstrated that strong sweep events were the dominant contributors to the Reynolds shear stress in the near-wall region, while ejections became the dominant contributor away from the wall. It was also observed that the peak location of the ejections and sweeps occur, respectively, in the higher and lower velocity regions of an embedded shear layer. Their results were in accordance with those presented by Gungor *et al.* (2016), who demonstrated that, for APG-TBLs, the ejections and sweeps dominate in the outer and near-wall regions, respectively. The quadrant splitting analysis was also used by Lozano-Durán *et al.* (2012), however in their work they extended this technique to a three dimensional perspective. In this work, the new proposal was carried out in a channel-flow and it was observed that most of the wall attached Q structures are related to sweeps or ejections and they are resposible for approximately 60% of the total content of the Reynolds shear-stress.

In the present work, a wall-resolved large-eddy simulation (LES) is performed to investigate the effect of APGs in a TBL developing on the suction side of a NACA0012 at 9 deg. angle of attack. The Reynolds and Mach numbers are $Re = 4 \times 10^5$ and $M = 0.2$, respectively. Tripping is applied at the leading edge on the suction side to guarantee the development of a fully turbulent boundary layer. Despite the high angle of attack, mean flow separation is not observed. The main objective of this work is to assess the presence of extreme events on the TBL and understand how such events are affected by the APG. Results are presented in terms of a quadrant analysis to assess the role of energetic coherent motions. We investigate the contributions of extreme events to sweep and ejection motions in the TBL, including their role in the Reynolds shear stress distribution.

2. NUMERICAL METHODOLOGY

A wall-resolved LES is employed to solve the non-dimensional compressible Navier-Stokes equations in general curvilinear coordinantes. A sixth-order accurate compact scheme is implemented on a staggered grid (Nagarajan *et al.*, 2003) to perform the spatial discratization of the governing equantions. An overset procedure is used in which an O-grid surrounds the airfoil and a Cartesian H-grid encloses the computational domain. The communication between the grids is done by using a fourth-order Hermite interpolation scheme in the overlapping zone (Bhaskaran and Lele, 2010). The solution is integrated in time integrated using an implicit second-order scheme in the O-grid, this method is used in order to reduce the stiffines problem of the fine resolution in the near-wall region. Moreover, a compact-storage third-order Runge-Kutta scheme is applied in the H-grid block.

A sixth-order compact filter (Lele, 1992) is applied in the flow region away from the airfoil surface to control numerical instabilities that may arise from grid stretching and interpolations between grids. The boundary conditions on the wall are defined as no-slip and adiabatic. In the far-field, characteristic boundary conditions based on Riemann invariants are employed together with a sponge layer that prevents reflection of acoustic waves. Furthermore, periodic boundary conditions are applied in the spanwise direction. The present numerical procedure described here has been validated for various simulations of compressible airfoil flows at different configurations (Wolf *et al.*, 2012a,b; Ricciardi and Wolf, 2022; Lui *et al.*, 2022; Miotto *et al.*, 2022). More details about the numerical procedure can be found in Nagarajan *et al.* (2003); Bhaskaran and Lele (2010), and Wolf (2011).

The simulation is performed for a NACA0012 airfoil at 9 deg. angle of attack, with a freestream Mach number $M = 0.2$ and Reynolds number based on the chord length and freestream velocity $Re = 4 \times 10^5$. A random spanwise and streamwise tripping is applied on the suction side from $0.04 \leq x \leq 0.09$, which is the region where the natural transition initiates. This tripping is applied in order to avoid the presence of Tollmien-Schlichting waves that would appear. In addition, the maximum amplitude of the tripping is chosen in such a way that a bypass transition occurs with a minimal disturbance to the flow. Due to tripping and the adverse pressure gradient, a turbulent boundary layer develops over the airfoil suction side, whereas a laminar boundary layer forms on the pressure side. It is important to mention that despite the high angle of attack, the TBL remains attached over the airfoil. Figure 1 presents a snapshot from the simulation where fine turbulent scales are shown along the airfoil and the inset highlights the region where the tripping is applied.

The O and H-grids have $1200 \times 170 \times 144$ and $960 \times 599 \times 72$ points, respectively, and the grid resolution is generated following the best practices in terms of wall-resolved LES (Georgiadis *et al.*, 2010). For the present simulation, the near-wall resolution in wall units is given by $\Delta x^+ < 40$, $\Delta y^+ < 0.50$ and, $\Delta z^+ < 16$. The airfoil span is chosen as 12% of the chord to resolve at least 5 times the length of the boundary layer displacement thickness at the trailing edge, minimizing effects of the periodic boundary conditions. More details about the flow conditions, tripping setup, and grid resolution can be found in Silva and Wolf (2024).

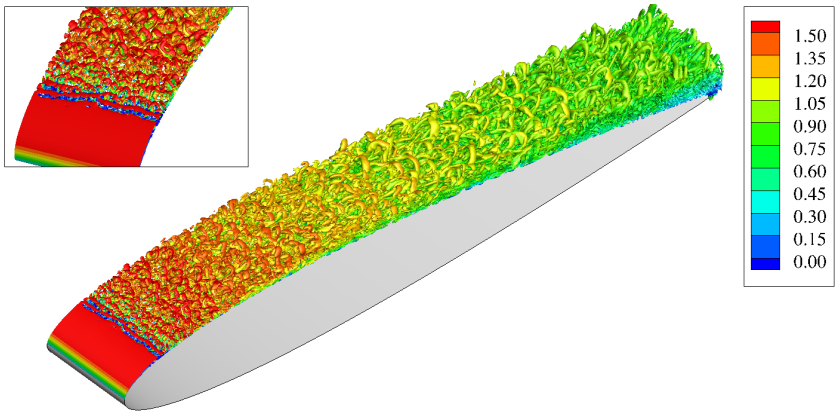

Figure 1. Isosurfaces of Q-criterion colored by tangential velocity normalized by the freestream velocity (U_t/U_∞) for the NACA0012 at 9 deg angle of attack, $Re = 4 \times 10^5$ and $M = 0.2$.

3. RESULTS

In this section, the effects of APG conditions ranging from mild to strong are evaluated along the TBL developing over a NACA0012 airfoil at 9 deg. angle of attack. The study consists on the application of a quadrant-splitting analysis where the impact of extreme events is evaluated in terms of the coherent motions sweeps and ejections. For the present simulation, such extreme events may be caused by the motion of energetic coherent structures, i.e., near-wall streaks and Kelvin-Helmholtz vortices, as was presented by Silva and Wolf (2024).

The pressure gradient parameter $\beta = \mathrm{dp/dx}(\delta^*/\tau_\mathrm{w})$ is plotted in Fig. 2, which presents the evolution of the APG over

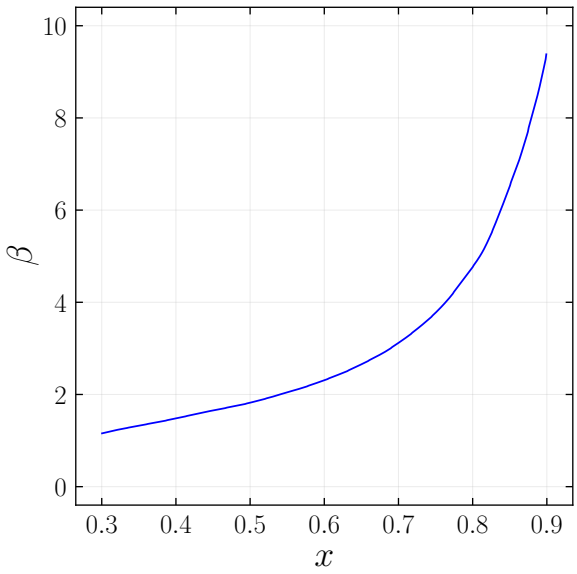

Figure 2. Chordwise evolution of the Rotta-Clauser pressure-gradient parameter β.

the airfoil suction side. Here, δ^* is the displacement thickness, τ_w is the wall shear stress and $\mathrm{d}p/\mathrm{d}x_\mathrm{t}$ is the streamwise pressure gradient. One can observe that this parameter presents a steep gradient downstream $x = 0.7$. Hence, special attention is given to results computed at chord positions $x = 0.5$, 0.7 and 0.9. The values of the pressure gradient paramenter for these positions are $\beta = 1.8$, 3.1 and 9.4, respectively. As one can see, conditions vary from mild to strong APGs, allowing an assessment of this parameter on the turbulent flow statistics.

3.1 Quadrant-splitting analysis

According to Robinson (1991), coherent motions in TBLs are major contributors to the Reynolds stress components and turbulence production. In this context, the motion of such structures are explored in terms of sweep and ejection events. Here, the analysis of these coherent motios is performed through a $u_t u_n$ quadrant splitting, in which u_t stands for the tangential velocity fluctuation and u_n for the wall-normal velocity fluctuation. This methodology was first proposed by Wallace *et al.* (1972) and Lu and Willmarth (1973) and allows the assessment of the ejection which are events related to Reynolds stress components residing in the second quadrant (Q_2), while sweep events appear in the fourth quadrant (Q_4).

In this work, the procedure employed by Schatzman and Thomas (2017) is considered, in which the quadrant analysis is implemented by using an identification function (ID) to determine the time instants when the velocity fluctuations u_t and u_n are located in a specific quadrant. Morevoer, we also verify if their product exceeds a predetermined threshold level H that determines the size of the hyperbolic hole presented in Fig. 3. The ID functions for Q_2 and Q_4 are determined as:

$$\mathrm{ID}_{Q_2}(t,H) = \begin{cases} 1 & \text{if } u_t(t) < 0 \text{ and } u_t(t)u_n(t) < -H\sqrt{\langle u_t^2\rangle}\sqrt{\langle u_n^2\rangle}\,, \\ 0 & \text{otherwise}\,. \end{cases} \tag{1}$$

$$\mathrm{ID}_{Q_4}(t,H) = \begin{cases} 1 & \text{if } u_t(t) > 0 \text{ and } u_t(t)u_n(t) < -H\sqrt{\langle u_t^2\rangle}\sqrt{\langle u_n^2\rangle}\,, \\ 0 & \text{otherwise}\,. \end{cases} \tag{2}$$

Figure 3 presents the $u_t(t)$ and $u_n(t)$ velocity fluctuation components at position $x = 0.9$ and wall-normal position $y^+ \approx 250$. In the figure, values of H ranging from 3 to 5 are displayed, and the color contours represent the joint probability density function (PDF) normalized by its maximum value. Large contributions to the Reynolds shear stress ($\langle u_t u_n\rangle$) are encountered in the components outside the hole, while small fluctuations are inside it. The latter, are related to the contribution of more quiescent periods as adressed by Lu and Willmarth (1973). For the location where this result is displayed in Fig. 3, the pressure-gradient parameter is $\beta = 9.4$ and the y^+ value corresponds to the position where a secondary peak is observed in the TKE production and Reynolds stresses (Silva and Wolf, 2024).

The contribution to the Reynolds shear stress from each quadrant taking into account a specific threshold parameter is

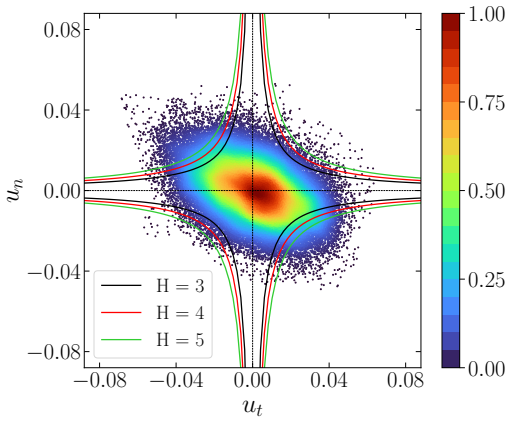

Figure 3. Tangential and wall-normal velocity fluctuations $u_t(t)$ and $u_n(t)$, respectively, measured at chord position $x = 0.9$, $y^+ \approx 250$. Color contours represent the joint PDF.

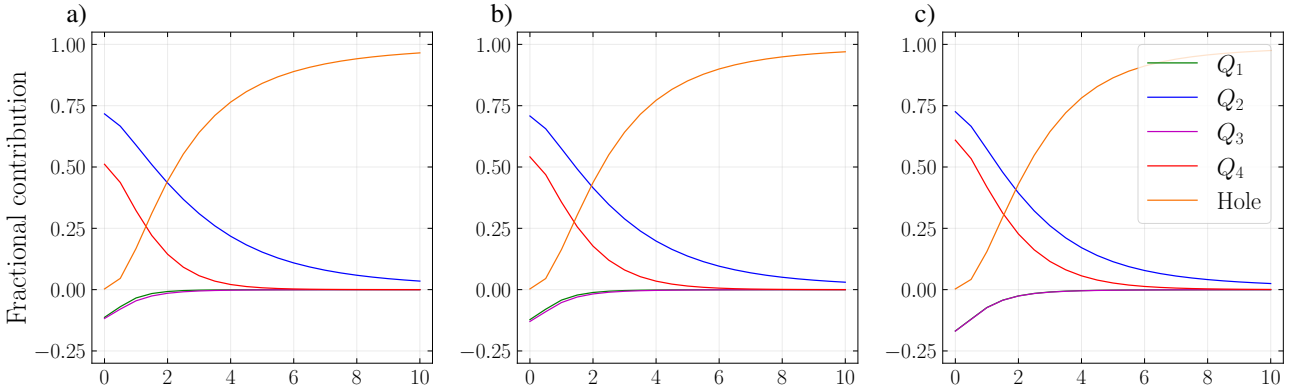

Figure 4. Fractional contribution of the individual quadrants to the Reynolds shear stress as a function of the threshold level H at chord positions (a) $x = 0.5$, (b) $x = 0.7$, and (c) $x = 0.9$.

determined by:

$$\frac{\langle u_t u_n \rangle_i (H)}{\langle u_t u_n \rangle} = \frac{1}{\langle u_t u_n \rangle} \lim_{T \to \infty} \frac{1}{T} \int_0^T u_t(t) u_n(t) \mathrm{ID}_{Q_i}(t, H) \mathrm{d}t \, . \tag{3}$$

Here, the subscript i refers to the $i-$th quadrant and T is the total sampling period. A analysis of the influence of the threshold level H is conducted and is presented in Fig. 4. In this figure, this analysis is presented for the airfoil chord positions $x = 0.5$, 0.7 and 0.9 considering the individual quadrants Q_i. It can be observed that the events related to the first and third quadrants (Q_1 and Q_3), related to inward and outward interactions, respectively (Lozano-Durán *et al.*, 2012), have less impact on the total Reynolds shear stress distribution, even for low threshold values. Although these interactions slightly increase with the APG as demonstrated in the figure for larger values of the chord position. On the other hand, the predominant contribution come from the sweeps (Q_2) and ejections (Q_4), with the former being more prominent. At downstream positions, where the APG is stronger (see Fig. 2), it can be observed that the sweeps increase their contribution to the total Reynolds shear stress. The figure also shows an orange line which depicts the Reynolds shear stress computed for the velocity fluctuations inside the hole. The present results demonstrate the influence of the pressure gradient on the contribution of each quadrant to the Reynolds shear-stress. However, it is important to mention that at each chord position, the TBL is subjected to different local Reynolds number. In addition to it, the evolution of the boundary layer over the airfoil (hystorical effects) is also an important feature to be considered. Therefore, it is important to highlight that these effects also contribute to the Reynolds shear-stress. Nevertheless, according to Monty *et al.* (2011), for moderate Reynolds numbers, the effects of pressure gradient are more relevant for the turbulence statistcs than those from the local Reynolds numbers.

In order to further evaluate the impact of sweeps and ejections on the Reynolds shear stress, Fig. 5 presents a comparison at $x = 0.5$, 0.7 and, 0.9 for thresholds $H = 3$, 4 and 5 represented by the different line styles. The present threshold parameters are chosen in order to verify the role of extreme events that contribute significantly to the turbulence statistics and boundary layer dynamics. Results are depicted along the wall-normal direction, where the solid black line represents the total Reynolds stress. Ejections and sweeps are represented by the blue and red lines, respectively. From the analysis of Fig. 5 one can see that the sweeps are the dominant coherent motion in the near wall region, while in the outer layer, the

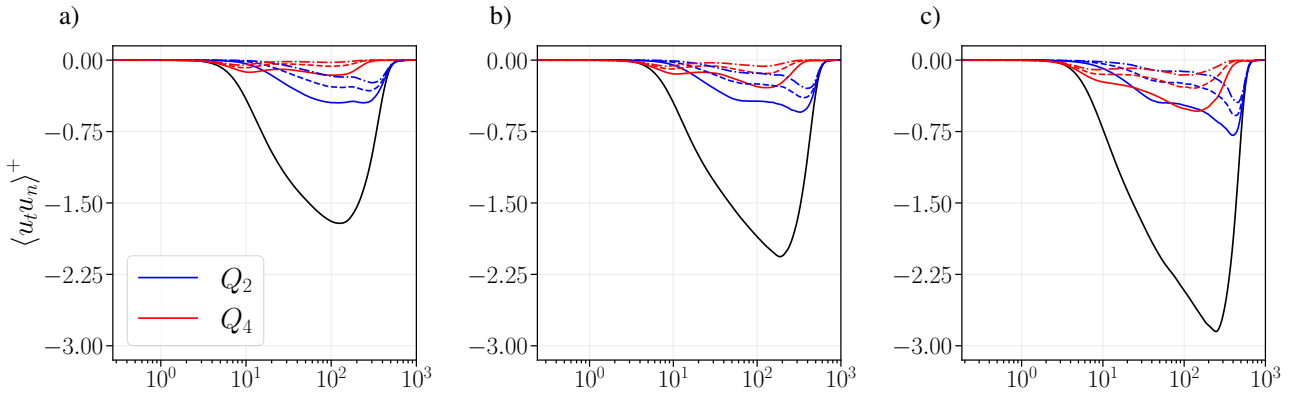

Figure 5. Contribution of ejections (Q_2) and sweeps (Q_4) to the Reynolds shear stress at chord positions (a) $x = 0.5$, (b) $x = 0.7$ and, (c) $x = 0.9$. The line styles indicate the magnitude of the threshold parameter (—) $H = 3.0$, (- -) $H = 4.0$, and (-·-) $H = 5.0$.

dominace is due to the ejections. For $x = 0.5$, the change in dominance occurs at $y^+ \approx 20$, where the ejections become a major contributor to the shear stress. In such cases, the contributions from ejections are concentrated further in the outer layer.

The same trend is observed for position $x = 0.7$ (Fig. 5(b)), however it can be observed that the contribution of sweeps (Q_4) starts to increase along the boundary layer thickness. In addition, one can see an emergence of an outer peak in the contribution coming from the ejections (Q_2). The results for the position $x = 0.9$ displayed in Fig. 5(c), in which, one can observe that the contribution of the sweeps is even higher. At the region $20 \lesssim y^+ \lesssim 200$, sweeps and ejections have similar contributions, displaying exchanges in the dominance of events. Moreover, the peak in the ejections is more evident in the region close to the boundary layer edge.

4. CONCLUSIONS

In the present work, a wall-resolved LES is conducted in order to investigate the APG effects on a TBL developing on the suction side of a NACA0012 airfoil with 9 deg. angle of attack. The flow conditions are set as Reynolds number based on the chord length and freestream velocity $Re = 4 \times 10^5$ and freestream Mach number $M = 0.2$. A quadrant analysis is presented to understand the role of extreme events in sweeps and ejections including their importance in the Reynolds shear stress distributions. This study demonstrates that, in the near-wall region, sweep events are the main contributor to the Reynolds shear stress while away from the wall, ejections are the dominant coherent motions. In addition, at downstream positions, where the pressure gradient parameter is higher, the presence of sweeps throughout the boundary layer is increased.

5. ACKNOWLEDGEMENTS

The authors acknowledge the financial support received from Fundação de Amparo à Pesquisa do Estado de São Paulo, FAPESP, under grants No. 2013/08293-7 and 2021/06448-0. FAPESP is also acknowledged for the scholarships provided to the first author under grants No. 2022/00256-4 and 2023/01657-5. The authors also thank Laboratório Nacional de Computação Científica (LNCC) and Centro Nacional de Processamento de Alto Desempenho em São Paulo (CENAPAD-SP) for providing the computational resources via SDumont and Lovelace clusters, where the numerical simulations were performed through projects SimTurb and 551, respectively.

6. REFERENCES

Bhaskaran, R. and Lele, S.K., 2010. "Large eddy simulation of free-stream turbulence effects on heat transfer to a high-pressure turbine cascade". *J. of Turbulence*, Vol. 11, pp. 1–15.

Farazmand, M. and Sapsis, T.P., 2017. "A variational approach to probing extreme events in turbulent dynamical systems". *Science Advances*, Vol. 3, p. e1701533.

Georgiadis, N.J., Rizzetta, D.P. and Fureby, C., 2010. "Large-eddy simulation: current capabilities, recommended practices, and future research". *AIAA Journal*, Vol. 48, pp. 1772–1784.

Gungor, A.G., Maciel, Y., Simens, M.P. and Soria, J., 2016. "Scaling and statistics of large-defect adverse pressure gradient turbulent boundary layers". *International Journal of Heat and Fluid Flow*, Vol. 59, pp. 109–124.

Lele, S.K., 1992. "Compact finite difference schemes with spectral-like resolution". *J. of Comput. Physics*, Vol. 103, pp. 16–42.

Lozano-Durán, A., Flores, O. and Jiménez, J., 2012. "The three-dimensional structure of momentum transfer in turbulent channels". *J. Fluid Mech.*, Vol. 694, pp. 100—130.

Lu, S.S. and Willmarth, W.W., 1973. "Measurements of the structure of the reynolds stress in a turbulent boundary layer". *Journal of Fluid Mechanics*, Vol. 60, No. 3, p. 481–511.

Lui, H.F.S., Ricciardi, T.R., Wolf, W.R., Braun, J., Rahbari, I. and Paniagua, G., 2022. "Unsteadiness of shock-boundary layer interactions in a Mach 2.0 supersonic turbine cascade". *Physical Review Fluids*, Vol. 7, p. 094602.

Miotto, R.F., Wolf, W.R., Gaitonde, D. and Visbal, M., 2022. "Analysis of the onset and evolution of a dynamic stall vortex on a periodic plunging aerofoil". *J. Fluid Mech.*, Vol. 938, p. A24.

Monty, J.P., Harun, Z. and Marusic, I., 2011. "A parametric study of adverse pressure gradient turbulent boundary layers". *International Journal of Heat and Fluid Flow*, Vol. 32, No. 3, pp. 575–585.

Nagarajan, S., Lele, S.K. and Ferziger, J.H., 2003. "A robust high-order compact method for large eddy simulation". *J. of Comput. Physics*, Vol. 191, pp. 392–419.

Ricciardi, T.R. and Wolf, W.R., 2022. "Switch of tonal noise generation mechanisms in airfoil transitional flows". *Physical Review Fluids*, Vol. 7, p. 084701.

Ricciardi, T.R., Wolf, W.R. and Taira, K., 2022. "Transition, intermittency and phase interference effects in airfoil secondary tones and acoustic feedback loop". *J. Fluid Mech.*, Vol. 937, p. A23.

Robinson, S.K., 1991. "Coherent motions in the turbulent boundary layer". *Annual Review of Fluid Mechanics*, Vol. 23, No. 1, pp. 601–639.

Schatzman, D.M. and Thomas, F.O., 2017. "An experimental investigation of an unsteady adverse pressure gradient turbulent boundary layer: embedded shear layer scaling". *J. Fluid Mech.*, Vol. 815, pp. 592–642.

Silva, L.J.O. and Wolf, W.R., 2024. "Embedded shear layers in turbulent boundary layers of a NACA0012 airfoil at high angles of attack". *International Journal of Heat and Fluid Flow*, p. 109353.

Wallace, J.M., Eckelmann, H. and Brodkey, R.S., 1972. "The wall region in turbulent shear flow". *Journal of Fluid Mechanics*, Vol. 54, No. 1, p. 39–48.

Willmarth, W.W. and Lu, S.S., 1972. "Structure of the reynolds stress near the wall". *J. Fluid Mech.*, Vol. 55, pp. 65—-92.

Wolf, W.R., 2011. *Airfoil aeroacoustics: LES and acoustic analogy*. Ph.D. thesis, Stanford University.

Wolf, W.R., Azevedo, J.L.F. and Lele, S.K., 2012a. "Convective effects and the role of quadrupole sources for aerofoil aeroacoustics". *J. Fluid Mech.*, Vol. 708, pp. 502—-538.

Wolf, W.R., Lele, S.K., Jothiprasad, G. and Cheung, L., 2012b. "Investigation of noise generated by a DU96 airfoil". In *18th AIAA/CEAS Aeroacoustics Conference (33th AIAA Aeroacoustics Conference), AIAA Paper 2012-2055*. pp. 1–15.

7. RESPONSIBILITY NOTICE

The authors are solely responsible for the printed material included in this paper.